Supplementary Information

Tuning the structure and photocatalytic performance of tri-s-triazine-based polyimides through temperature-controlled imidization

Renan F. Bez [a,*], Luisa I. Fusinato [b,c], Vinícius Glitz [d], Felipe L. Marino [a], Camila P. Magrin [e], Ricardo A. F. Machado [c], Gustavo A. Micke [e], Renato L. T. Parreira [f], Giovanni F. Caramori [d], François Perreault [b], Adriana P. Gerola [a,*]

[a] *Laboratório de Catálise e Fenômenos Interfaciais - LACFI, Department of Chemistry, Federal University of Santa Catarina (UFSC), Florianópolis, 88040-900, Brazil*
[b] *Department of Chemistry, Faculty of Sciences, University of Québec in Montréal, H2L 2C4, Montréal, Canada*
[c] *Laboratório de Controle e Processos de Polimerização, LCP, Department of Chemical Engineering, Federal University of Santa Catarina (UFSC), Florianópolis, 88040-900, Brazil*
[d] *Grupo de Estrutura Eletrônica Molecular e Materiais, GEEMM, Department of Chemistry, Federal University of Santa Catarina (UFSC), Florianópolis, 88040-900, Brazil*
[e] *Laboratório de Eletroforese Capilar e Cromatografia - LabECC, Department of Chemistry, Federal University of Santa Catarina (UFSC), Florianópolis, 88040-900, Brazil*
[f] *Research Center in Exact and Technological Sciences, University of Franca, Franca, 14404-600, Brazil*

* E-mail: adriana.gerola@ufsc.br, renanfbez@gmail.com

Contents

S1. Experimental details

S1.1. Chemicals and TPIs samples details

Melamine (99%, Sigma-Aldrich), 1,4,5,8-naphthalenetetracarboxylic dianhydride (NTCDA, 98%, Sigma-Aldrich), pyromellitic dianhydride (PMDA, 97%, Sigma-Aldrich), methyl orange (MO, Merck), 2,4-dichlorophenoxyacetic acid (2,4-D, Sumitomo Chemical), acetone P.A. (Synth), ethanol P.A. (Synth), methanol P.A. (Vetec), anhydrous sodium sulfate P.A. (Na_2SO_4, Neon), N-tert-butyl-α-phenylnitrone (PBN, Sigma-Aldrich), 5,5-dimethyl-1-pyrroline N-oxide (DMPO, Sigma-Aldrich) were commercially purchased and used without prior purification.

Table S1. Melting points of anhydride precursors and polymerization temperatures for TPIs synthesis

Polyimide	Sample name	melem MW (g mol^{-1})	Anhydride MW (g mol^{-1})	Anhydride mp (°C)	Polymerization temperature (°C)
melem-PMDA	**MP**	218.18	218.12	286.9	250, 275, 300 and 325
melem-NTCDA	**MN**		268.18	322.1	275, 300, 325 and 350

S1.2. Light source

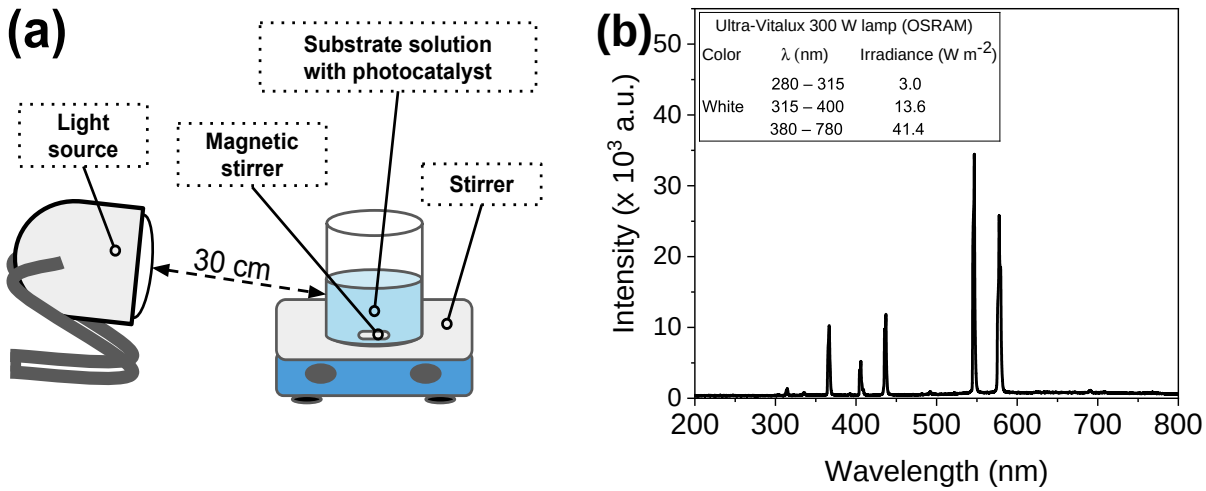

Fig. S1. (a) Schematic of the setup employed for the photodegradation tests, and (b) emission spectrum and main operating specifications of the light source used in this work.

S1.3. Photocatalytic 2,4-D degradation

The photodegradation of the 2,4-D herbicide was carried out under the same photocatalytic system applied in MO tests. In detail, 50 mg of photocatalyst was dispersed in 60 mL of 2,4-D solution (12 ppm, pH = 6.0 ±0.5) and kept in the dark under continuous stirring for 60 min to reach adsorption–desorption equilibrium. Following the initiation of irradiation, aliquots were collected every 30 min, centrifuged at 750 rpm for 30 min, and the supernatant was analyzed. The change in 2,4-D concentration was monitored using high-performance liquid chromatography (HPLC, 1200 Series, Agilent) coupled with a mass spectrometry (MS/MS) system equipped with a triple quadrupole mass analyzer (Q Trap 3200, Applied Biosystems/MDS Sciex), operated in negative electrospray (TurboIonSpray, Applied Biosystems/MDS Sciex) ionization mode. Multiple reaction monitoring (MRM)

consisted of tracking the 219.0/160.4 and 219.0/125.0 m/z transitions for quantification and confirmation, respectively. The separation was performed on a Synergi 4μ Polar-RP column (80 Å, 150 x 2.00 mm). The mobile phase consisted of (A) water with formic acid 0.1 % (v/v) and (B) methanol (Table S2).

Table S2. Mobile phase gradient used in HPLC for the determination of 2,4-D concentration

Time (min)	**A (%)**	**B (%)**
0.0	90	10
2.0	90	10
7.0	10	90
12.0	10	90
20.0	40	60

S2. Structural and electronic characterization

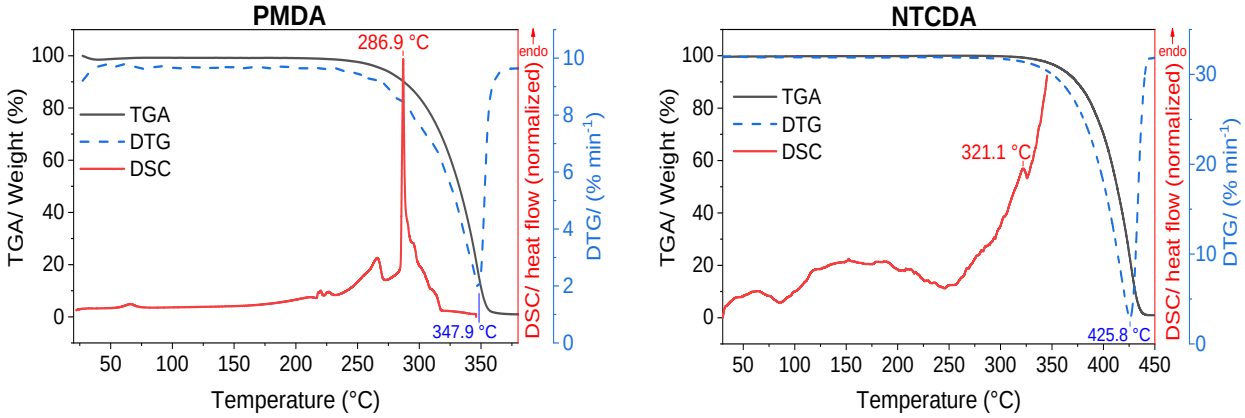

Fig. S2. TGA, DTG and DSC curves for PMDA and NTCDA anhydrides.

Table S3. Main PI bands identified by FTIR and their attribution

	Wavenumber (cm^{-1})	
	MP	**MN**
ν(C–N) ν(C=N)	1350-1650	
σ(C–N)	803	
ν(N–H)	3475; 3426	3486; 3426
ν(C=O)	1774; 1730	1860; 1777
ν(C–N–C)	1370	1355
σ(C=O)	720	735

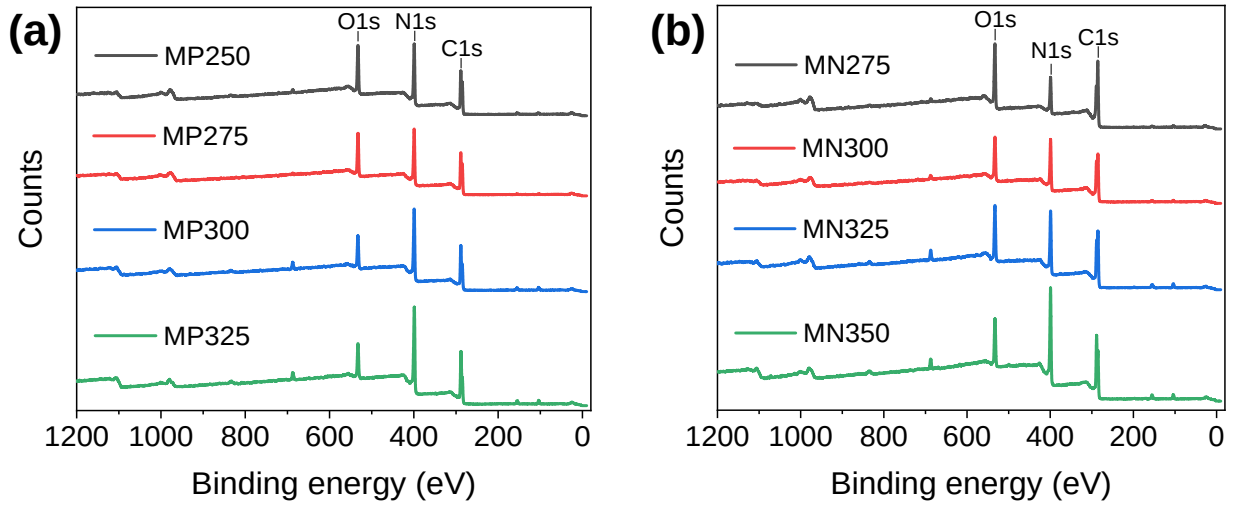

Fig. S3. Survey XPS spectra of (a) MP, and (b) MN TPIs.

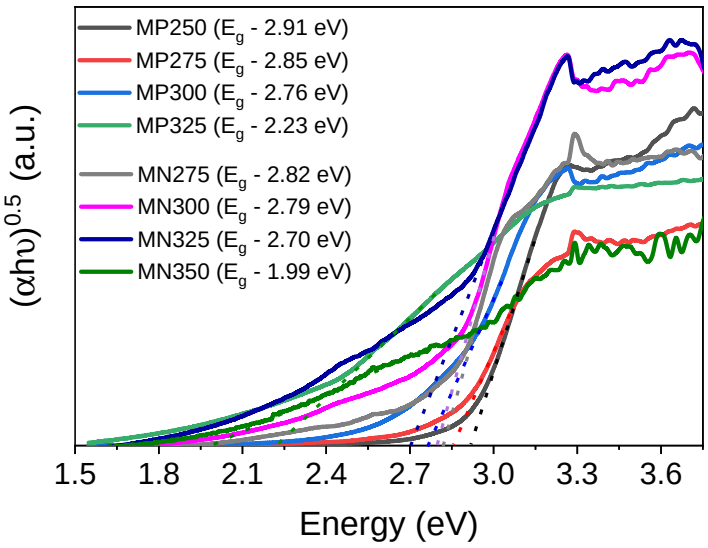

Fig. S4. Tauc plot and calculated band gap energies.

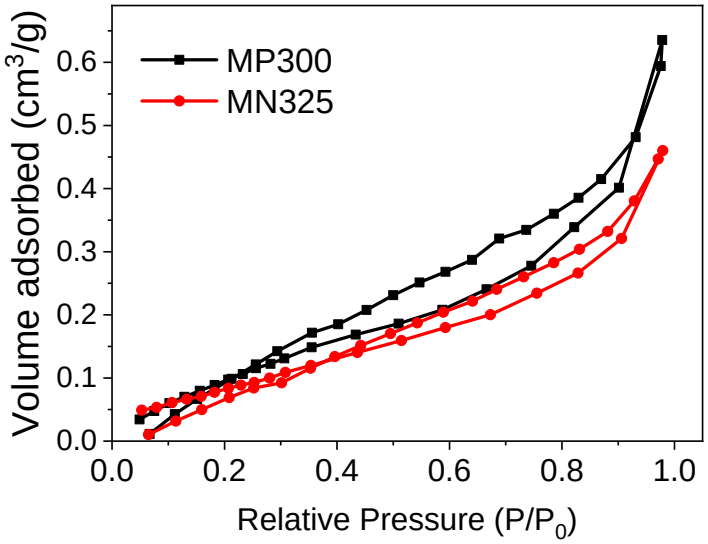

Fig. S5. N_2 adsorption/desorption isotherm curves of the MP300 and MN325 TPIs.

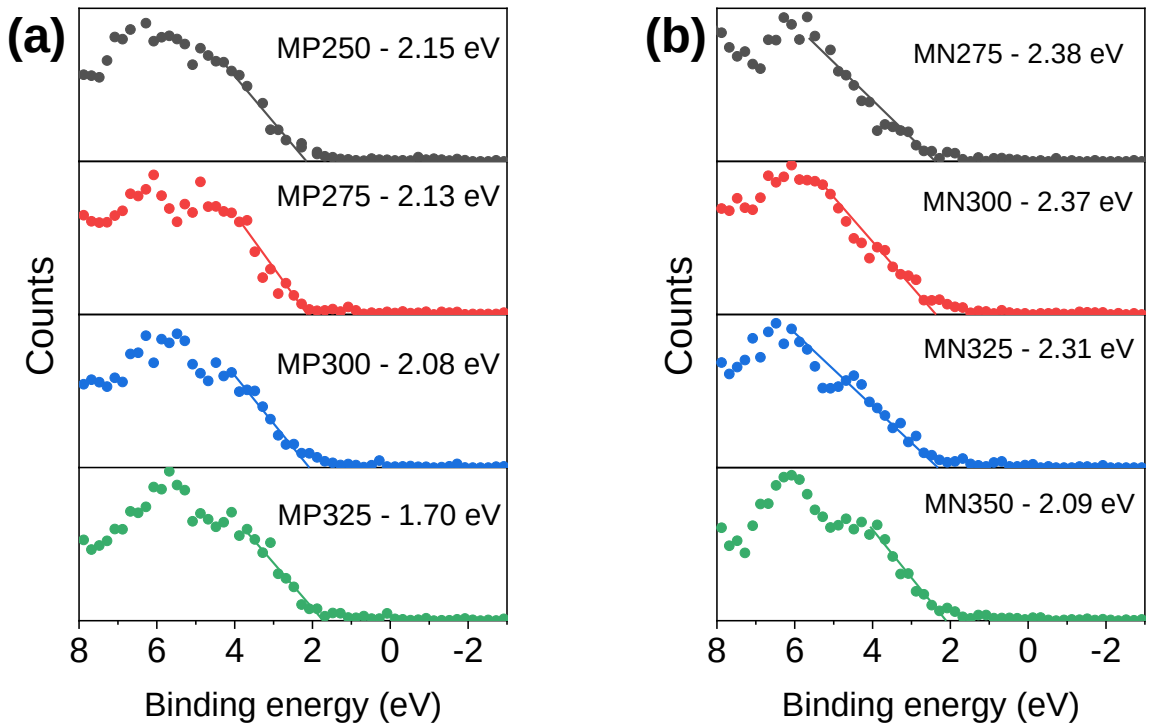

Fig. S6. VB-XPS spectra of (a) MP and (b) MN TPIs.

S3. Electronic structure calculations

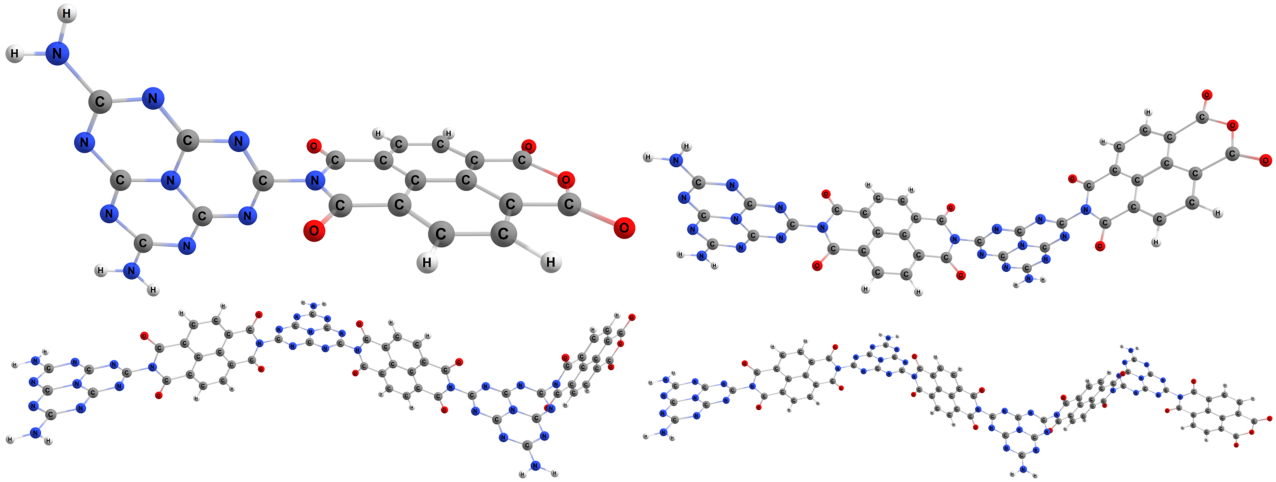

Fig. S7. Minimum-energy structures obtained for the MN:1, MN:2, MN:3, and MN:4 systems at the BP86/def2-TZVP level of theory in the gas phase.

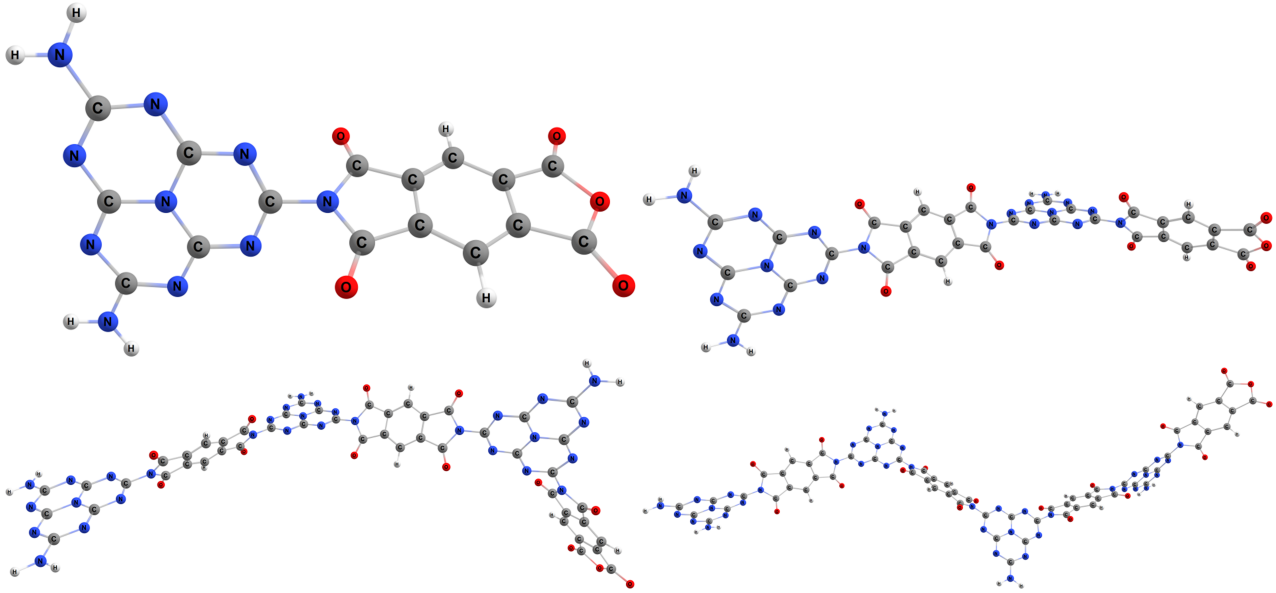

Fig. S8. Minimum-energy structures obtained for the MP:1, MP:2, MP:3, and MP:4 systems at the BP86/def2-TZVP level of theory in the gas phase.

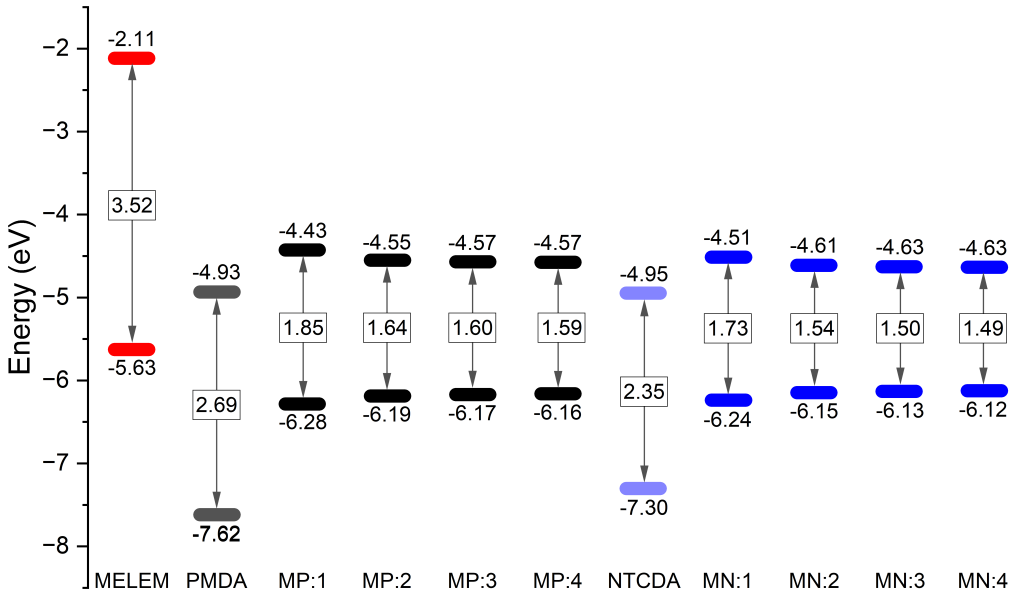

Fig. S9. Energy level for calculated species at the BP86/def2-TZVP level of theory in the gas phase.

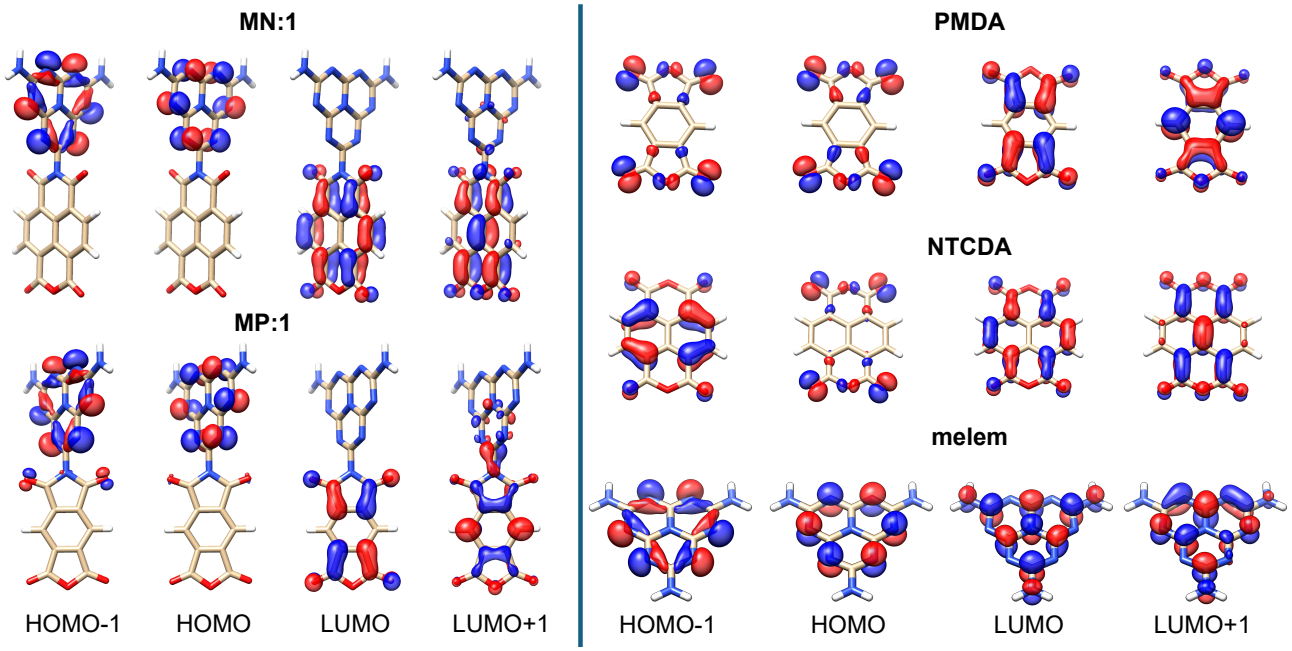

Fig. S10. Frontier orbitals for the MN:1 and MP:1 and the melem, PMDA, and NTDA monomers at the BP86/def2-TZVP level of theory in the gas phase.

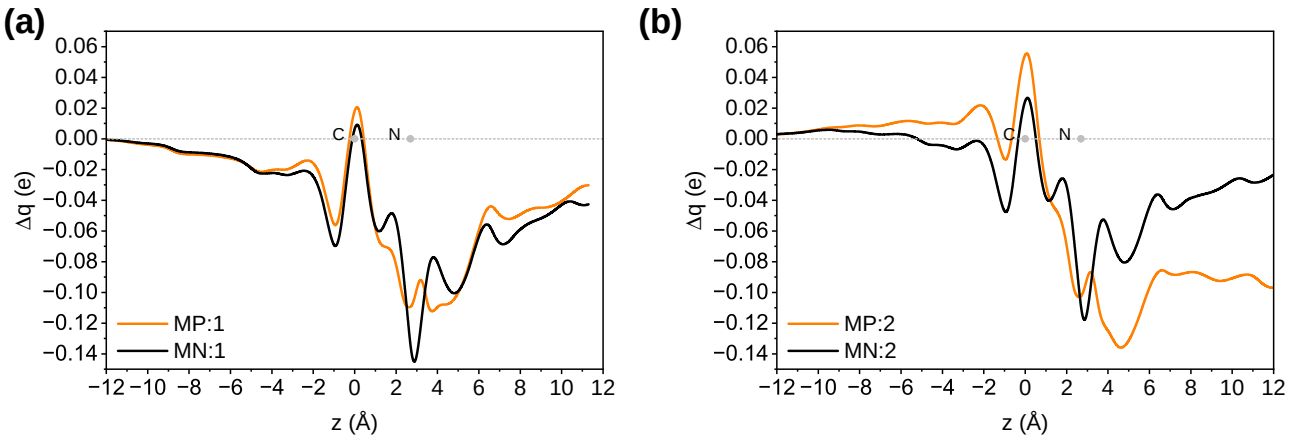

Fig. S11. Charge displacement analysis for the oligomers: (a) MP:1 and MN:1, and (b) MP:2 and MN:2.

S4. Photocatalytic degradation

S4.1. Kinect studies of methyl orange photodegradation

The kinetics of the methyl orange (MO) photocatalytic degradation reactions were evaluated using the pseudo-first-order model: $-ln\left(\frac{C_t}{C_0}\right) = kt$; where k is the pseudo-first-order rate constant, which corresponds to the fitting line slope, C_0 is the initial concentration of MO solution after the adsorption–desorption process and C_t represents the concentrations at time t.

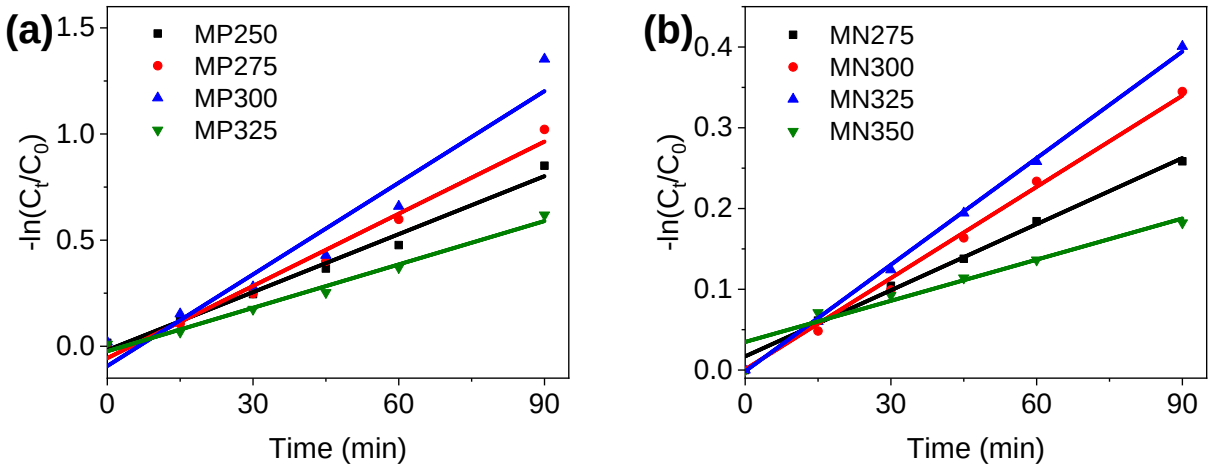

Fig. S12. Pseudo-first-order reaction kinetics for (a) MPs and (b) MNs in MO photodegradation experiments.

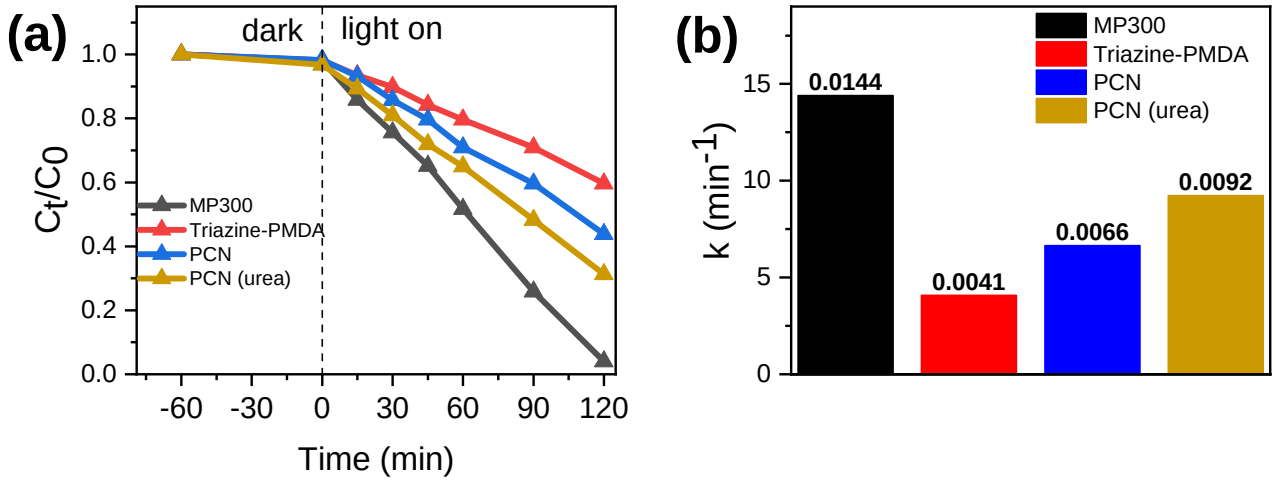

Fig. S13. (a) Comparison of the MO photodegradation efficiencies of PCN (derived from urea and melamine), triazine–PMDA PI, and MP300; and (b) the corresponding k values.

S4.2. Reuse tests for MO photodegradation

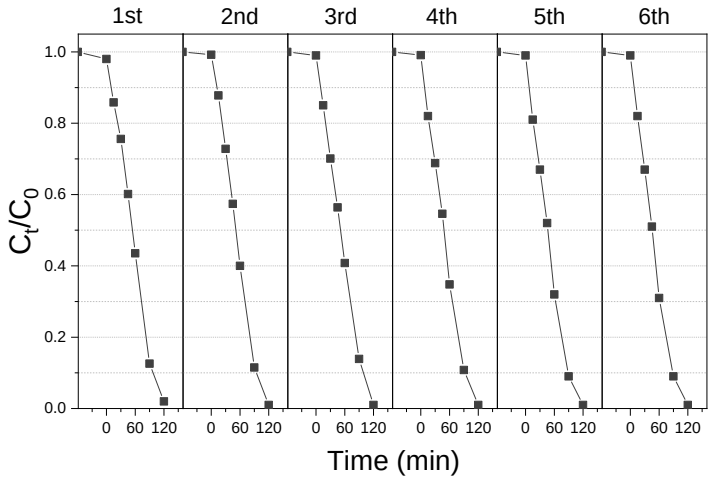

Fig. S14. Reusability tests for MP300 in the photodegradation of MO under white light.

S4.3. 2,4-D photodegradation experiments

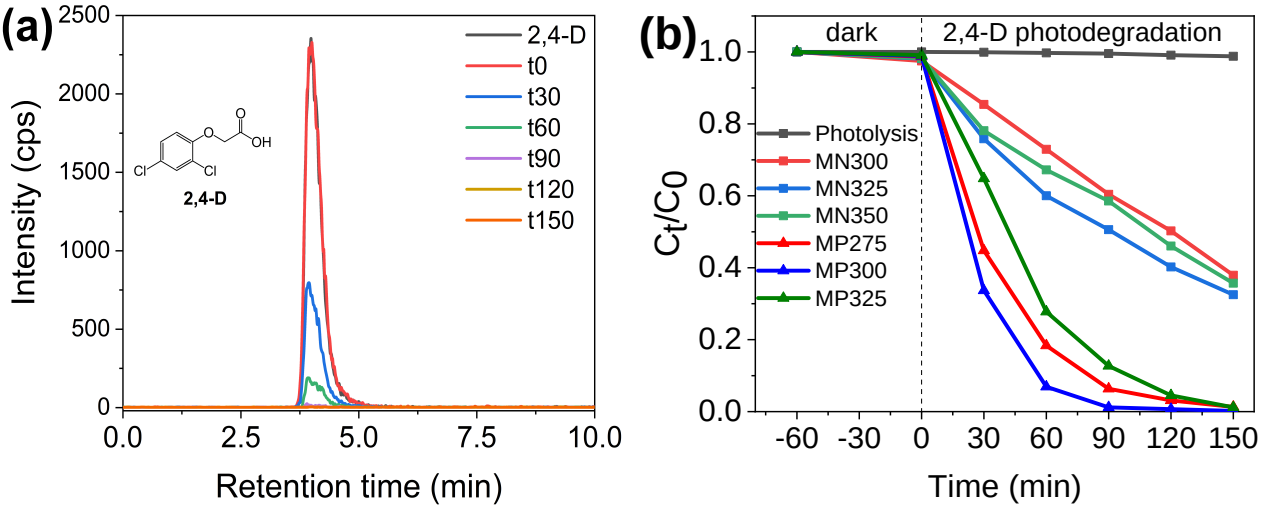

Fig. S15. (a) Chromatograms of herbicide 2,4-D obtained before and after different irradiation times (min) during photocatalytic tests using the MP300 sample, and (b) corresponding C_t/C_0 profiles for 2,4-D photodegradation over different TPIs.

S5. EPR analysis

S5.1. Solid-state EPR

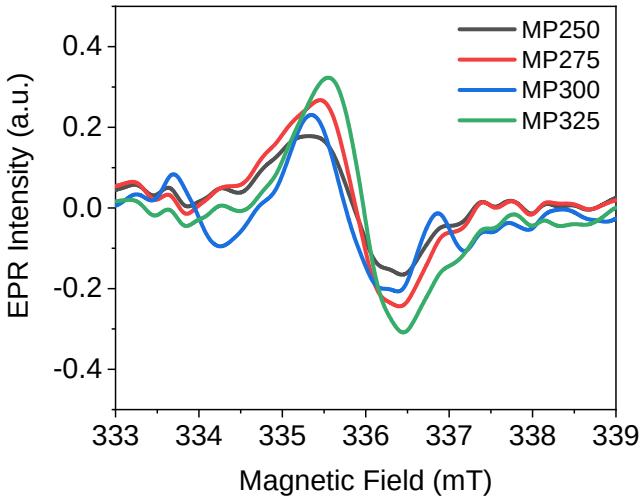

Fig. S16. Solid-state EPR spectra of MP PIs.

S5.2. Evaluation of reactive species

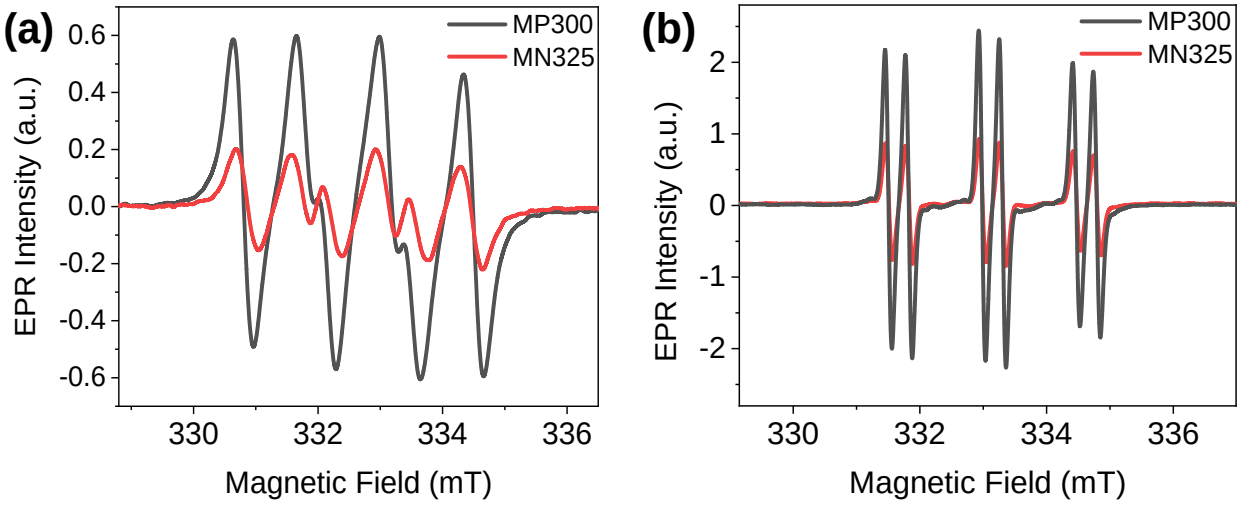

Fig. S17. EPR spectra of MP300 and MN325 after 5 min irradiation using (a) DMPO (0.02 mol L^{-1}; methanol) and (b) PBN (0.1 mol L^{-1}; 1:1 H_2O:ethanol) as spin-trapping agents.